PHYSICAL REVIEW D VOLUME 17, NUMBER 4 15 FEBRUARY 1978

Derivation of dual models from field theory. II

Charles B. Thorn

Center for Theoretical Physics, Laboratory for Nuclear Science and Department of Physics, Massachusetts Institute of Technology, Cambridge, Massachusetts 02139

(Received 23 November 1977)

We rewrite $\lambda\phi^4$ theory as a dual string expansion by performing a combined topological strong-coupling expansion on an x^+, P^+ lattice. The resulting expansion is the standard dual loop expansion plus the point-energy-momentum density graphs of Green. The expansion goes through only for the "wrong" sign of λ, i.e., when the theory is asymptotically free and infrared unstable. The coupling strength λ is fixed by an eigenvalue condition, and the rest tension of the string, T_0, replaces it as a free parameter. The continuum limit only exists for the critical dimension $D = 26$. We suggest that this approach might be a suitable starting point for spectrum calculations in quantum chromodynamics.

I. INTRODUCTION

In a recent letter,[1,2] hereafter referred to as (I), we reported a precise connection between field theory and dual resonance models based on a combined strong-coupling and topological expansion. Here we give a more complete account of these results, including detailed derivations omitted from the letter version.

The history of attempts to identify dual resonance models (DRM) as an approximation to field theory is nearly as long as that of dual models. Nielsen and Olesen and, independently, Sakita and Virasoro[3] suggested in 1970 that DRM were approximations to very large planar Feynman diagrams ("fishnet" diagrams). The motivation for this idea was that in a strong-coupling theory diagrams with many vertices should dominate. What was lacking at that time was (1) a justification for the planar approximation and (2) a systematic method of calculating higher-order corrections to the leading fishnet diagram. The calculation done by these authors assumed that propagators could be well approximated by Gaussian functions in momentum space, and it was not clear how this approximation could be systematically carried out.

In the meantime much progress was made in understanding the basic dynamics underlying the DRM.[4] The spectrum of the DRM was shown to be that of a relativistic string,[5] and the dual resonance amplitudes were shown to be consequences of the ansatz that the probability amplitude for a string to break in two was proportional to the overlap of wave functionals of the three strings involved in the process.[6] The crucial ingredient to the solution of these problems was the discovery[5] that string dynamics simplifies dramatically when referred to an infinite-momentum frame (light-cone quantization).

In 1974 't Hooft[7] utilized this discovery to make the fishnet-diagram idea more precise. He observed that when the Feynman propagators are written in a mixed $x^+, P^+, \vec{x}_\perp$ representation[5] [$V^\pm = (1/\sqrt{2})(V^0 \pm V^3)$], large planar Feynman diagrams resemble very closely the string functional integrals introduced by Mandelstam.[6] The connection was not exact, however, and 't Hooft suggested that the string calculations might be approximations to the sum over all planar diagrams. In the same paper 't Hooft also lent some insight into the nature of the planar approximation by observing that planar diagrams become more important as S, the size of the symmetry multiplets of a field theory, gets larger. Indeed, in the limit $S \to \infty$ with $g^2 S$ fixed, only planar diagrams survive. Subsequent developments along these lines centered around this latter observation. In particular, Veneziano[8] and others have developed qualitative dynamical schemes based on $1/S$-type expansions. Central to these schemes is the assumption that the leading order in $1/S$ is qualitatively identical to the DRM.

In I we clarified the sense in which the DRM is an approximation to the sum over planar graphs. We showed that by making x^+ and P^+ discrete, i.e., putting these variables on a two-dimensional lattice, one could define a topological strong-coupling expansion of $\lambda\phi^4$ theory in which the leading order approached precisely the DRM in the continuum limit. Further, a large subset of nonleading diagrams could be mapped one to one onto the lattice string diagrams of Giles and Thorn.[9] The remaining nonleading diagrams could be identified in the continuum limit as the point energy-momentum insertions which Green[10] has suggested must be added to the standard dual loop expansion if pointlike behavior at short distances is to be achieved. The present article is devoted to a detailed exposition of the work reported in I.

Before proceeding to this task, we should perhaps explain some of the motivations for this pro-

gram of investigation. The DRM is the only example of an extended model of hadrons, which is consistent with Lortenz invariance, quantum mechanics, crossing symmetry, Regge behavior, and unitarity. Other types of extended models, such as the MIT bag model, may be more flexible phenomenologically, but they have not yet been consistently quantized. Thus the DRM remains an important theoretical testing ground for the viability of such models.

The dual model has serious shortcomings, however, and the identification we have achieved tells us what aspects of field theory are *left out* of the dual approximation. At the same time it instructs us precisely how they are to be incorporated if we wish to have a better approximation. Such improvements may well have to be made nonperturbatively, e.g., to finite order in the dual expansion there are negligible high-momentum components in the hadronic wave functions.

Another virtue of our derivation of dual models from field theory is that it teaches us how to incorporate internal symmetry in dual models. Previously this could only be done in an *ad hoc* manner. Now one can *calculate* the dual model associated with a field theory with arbitrary internal-symmetry structure. In particular one may attempt the dual approximation to quantum chromodynamics (QCD), the current favorite theory of strong interactions. Of course, this approximation neglects such things as high-momentum constituents, but it may give a tolerable approximation to the level structure of the theory. It may also give us insight into the spontaneous symmetry breaking of chirality.

Finally, the DRM is a model whose consistency depends on severe restrictions on degrees of freedom. For example, the generalized Veneziano model works only if there are $26-D$ additive conserved quantum numbers, where D is the dimension of space-time. It may be that the number of hadronic flavors is constrained by self-consistency. Our work with field theory reveals the nature of these restrictions; the expansion can be carried out only if the system is critical and this demands that the system have a definite number of degrees of freedom. A true unification of weak, electromagnetic, and strong interactions may require that these constraints be taken into account.

II. THE DUAL STRING EXPANSION OF $\lambda\phi^4$ FIELD THEORY

The starting point of our dual string expansion is the Feynman graph expansion for Green's functions written in an x^+, P^+ representation. Thus we write $[x^\pm = (1/\sqrt{2})(x^0 \pm x^{d+1}),\ P^\pm = (1/\sqrt{2})(P^0 \pm P^{d+1})]$

$$D_F(x) \equiv \frac{-i}{(2\pi)^{d+2}} \int d^{d+2}P \frac{\exp[i(\vec{x}_\perp \cdot \vec{p}_\perp - x^- P^+ - x^+ P^-)]}{\vec{P}_\perp^{\,2} + m^2 - 2P^+P^- - i\epsilon}$$

$$= \frac{1}{(2\pi)^{d+1}} \int \frac{dP^+}{2|P^+|} \int d\vec{P}_\perp \theta(x^+P^+) \exp\{i[x_\perp \cdot \vec{P}_\perp - x^- P^+ - x^+[(\vec{P}_\perp^{\,2} + m^2)/2P^+]\}. \tag{2.1}$$

In the null-plane description,[11] it is useful to distinguish Feynman diagrams which have different x^+ ordering, even though they have identical topology. This distinction is possible because of the $\theta(x^+P^+)$ in (2.1). The region $x^+, P^+ > 0$ is disjoint from the one $x^+, P^+ < 0$. We may therefore adopt the convention that every line propagates forward in x^+. With this convention the propagator associated with any line is (after a Wick rotation $x^+ = -i\tau$, $\tau > 0$, $D = d + 2$)

$$D_F(\tau, P^+, \vec{x}_\perp) = \frac{dP^+}{4\pi P^+} \theta(P^+) \left(\frac{P^+}{2\pi\tau}\right)^{d/2} \times \exp[-(P^+/2\tau)\vec{x}_\perp^{\,2} - \tau m^2/2P^+]. \tag{2.2}$$

Each vertex will have the factors

$$V = \lambda \int d\tau \int d\vec{x}_\perp 2\pi\delta\left(\sum_i P_i^+\right), \tag{2.3}$$

where it is understood that the range of τ integration is restricted by the requirement that every line propagate forward in τ. Note that $\lambda > 0$ corresponds to a *negative* potential energy, $\lambda < 0$ to a positive potential energy.

A. The τ, P^+ Lattice

In I we proposed that Feynman diagrams be analyzed on a τ, P^+ lattice obtained by replacing all integrals over τ and P^+ by sums:

$$\tau = ka, \quad \int d\tau \to a \sum_k, \quad (k = 1, 2, \ldots);$$

$$P^+ = la\dot{T}_0, \quad \int dP^+ \to aT_0 \sum_l, \quad (l = 1, 2, \ldots).$$

The parameter T_0 has dimensions of force and will be identified as the rest tension of the string. Here it is the ratio of the minimal unit of P^+ (an infrared cutoff) to the minimal unit of τ (an ultraviolet cutoff). The propagator and vertex become

$$D_{lk}(\vec{x}_\perp) = \sum_{l>0} \left(\frac{T_0 l}{2\pi k}\right)^{d/2} \times \exp[-(T_0 l/2k)\vec{x}_\perp^{\,2} - km^2/2lT_0],$$

$$V = \lambda \sum_k \int d^d\vec{x}_\perp \frac{2\pi}{T_0} \delta_{l_f, l_i} \prod_{i=1}^{4} \frac{1}{(2l_i)^{1/2}} \left(\frac{1}{2\pi}\right)^2,$$

where δ_{l_f, l_i} is a Kronecker δ function, and we have redistributed some factors among propagator and vertex. Notice that the dependence on the lattice spacing, a, disappears. Conventional perturbation theory is regained by ordering the graphs contributing to a particular Green's function starting with those with the smallest number of vertices. Our lattice regulates all divergences. If $D \leq 4$, the continuum limit will exist order by order in perturbation theory as one can absorb all divergences into redefinitions of the coupling constant as in conventional renormalization theory.

B. The strong-coupling expansion

Our strong-coupling expansion is set up in the following way. Focus on a Green's function which spans $(N+1)$ a units of τ and carries MaT_0 units of P^+. Then because of the lattice, there are a maximal number of interactions which can occur, roughly $M(N+1)$. There are, of course, many graphs with this maximal number of vertices. The strong-coupling expansion is obtained by calculating the maximal graphs first and ordering the remaining graphs in a power series in $1/\lambda$. This straight strong-coupling expansion is formidable because the number of graphs of leading order proliferates. One way to organize all these graphs in the continuum limit is the dual string expansion to which we now turn.

The organizing principle of the dual string expansion is to calculate "planar" graphs first, and then to arrange the rest of the graphs according to their topology, replacing all planar subgraphs by the results of the "planar" calculation. We define a planar graph as one which can be drawn on a cylinder with no handles and which has no crossed lines. Note that the τ ordering of vertices may force a graph to have crossed lines and hence be nonplanar for our null-plane description, even though other τ orderings would be planar. Such exceptions only apply when some of the crossed lines are external. We include a cylindrical topology as planar. We have dubbed our expansion the dual string expansion to distinguish it from the standard dual loop expansion as the latter is included in but does not exhaust the former.

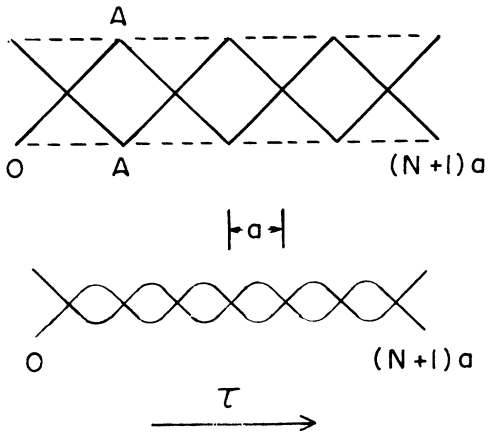

FIG. 1. Two ways of drawing the bare closed-string propagator carrying only two units of P^+. Each line carries $P^+ = aT_0$. The vertices on the dashed lines labeled A are identified.

C. The dual loop expansion (DLE)

We first identify all the graphs which exhaust the standard dual loop expansion. These are characterized by the requirement that *every line carries the minimal amount*, aT_0, *of* P^+. In the following, the total P^+ entering any graph is MaT_0.

1. *The bare closed-string propagator, M even.* See Figs. 1–3. First define the $M=2$ propagator as in Fig. 1. Then define the general M-even case as that unique planar graph spanning a fixed τ interval with a maximal number of vertices, and not containing subgraphs like Fig. 1. A typical case $M=6$ is shown in Fig. 2 where the dashed lines are identified. Note that for fixed M and

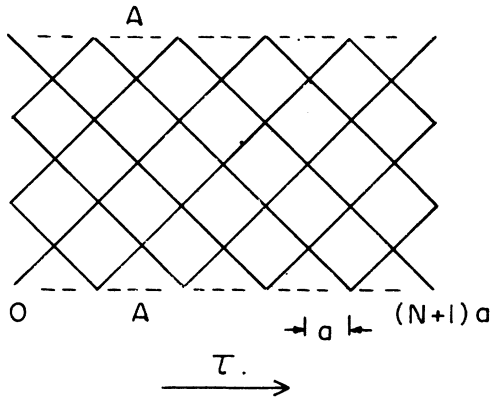

FIG. 2. Typical bare closed-string propagator carrying $M=6$ units of P^+. The dashed lines A are identified.

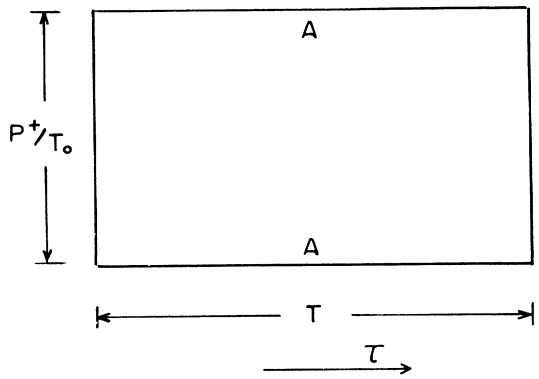

FIG. 3. The continuum limit of the closed-string propagator: M, $N \to \infty$ with $(N+1)/M - TT_0/P^+$ fixed. The lines are identified.

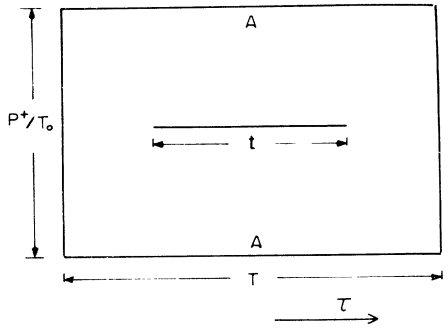

FIG. 5. The continuum limit of Fig. 4: M, N, $n \to \infty$ with $(N+1)/M = TT_0/P^+$ and $n/(N+1) = t/T$ fixed. The lines A are identified.

propagation time $(N+1)a$ these graphs contribute to leading order in the *strong-coupling expansion of planar graphs*. If we regard $M=2$ closed-string subgraphs as limiting cases of handles, the closed-string propagator *is* the $\lambda \to \infty$ limit of the sum of all planar graphs. The continuum-limit string graph is shown in Fig. 3.

2. *The open-string propagator.* This is most easily defined by considering a sequence of missing vertices in the closed-string propagator (see Figs. 4 and 5). Between times 0 and na an open string propagates so we identify (Fig. 6) as the open-string, even-M, propagator. This graph is $O((1/\lambda)^{(N+1)/2})$ compared to the closed-string propagator with the same M. We thus see that $-\frac{1}{2}\ln\lambda$ is a contribution to the energy of the open string. Clearly, we must have $\lambda > 0$ for real energies. We shall discuss this point a little later. Note in Fig. 8(a), the $M=2$ open string. Open strings with odd M are obtained by considering a sequence of missing vertices in the even-M open-string propagator (see Fig. 7). Note that a single line is the shortest open string [Fig. 8(b)], and the continuum limit is shown in Fig. 9. From Fig. 4 we also identify the following:

3. *The-closed-string–open-string vertex.* See Fig. 10 and similarly note the following:

4. *The three-open-string vertex.* See. Fig. 11.

To complete the list of ingredients for the dual loop expansion, we note also the definition of the following:

5. *The three-closed-string vertex.* See Fig. 12.

6. *The four-string vertex.* See Fig. 13.

7. *The closed-string emission vertex from an open string.* See Fig. 14.

The dual loop expansion for a specific scattering process may be written in terms of the light-cone interacting string graphs of Mandelstam.[6] Each such graph is an integral over the τ and σ coordinates of the various vertices included in the graph. For all τ and σ coordinates away from the end points, the integrand may be arbitrarily well approximated by the corresponding fishnet graph constructed from the above seven ingredients.

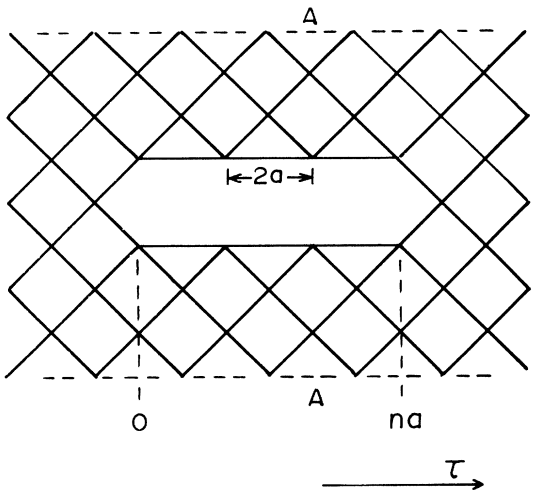

FIG. 4. A series of missing vertices in the closed-string propagator. Between times 0 and na an open-string propagates. The dashed lines A are identified.

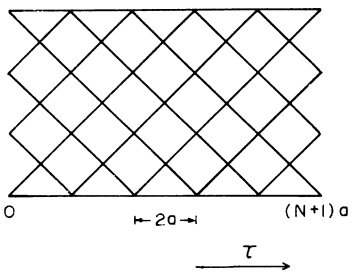

FIG. 6. The bare open-string propagator carrying $M=8$ units of P^+. Each line carries $P^+ = aT_0$.

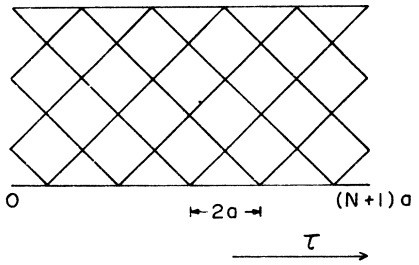

FIG. 7. The bare open-string propagator carrying $M=7$ units of P^+.

For τ and σ coordinates near the end points of integration the continuum limit is singular, and this is reflected in divergences of the τ and σ integrals.

The sum of all planar, minimal-P^+, Feynman graphs defined with our τ, P^+ lattice may be regarded as a lattice approximation to the sum of all planar interacting string graphs as in Giles and Thorn.[9] The fishnet graphs regulate the divergences at τ, σ end points, and away from the end points approach the correct expressions in the continuum limit. The end points are very sensitive to the detailed microscopic structure of the fishnet sum and depend explicitly on the lattice spacing. An important consistency requirement on the dual loop expansion is that all this detailed lattice dependence can be lumped into a renormalization of T_0 as $a \to 0$.[12]

Nonplanar, minimal-P^+, Feynman graphs may similarly be regarded as a lattice version of corresponding nonplanar dual graphs, and again all the detailed microscopic structure must be shown to only renormalize T_0 as $a \to 0$. If the final result of a calculation is expressed in terms of the renormalized T_0 the continuum limit will be finite and independent of microscopic details. This renormalizability has apparently been shown for the ultraviolet ($\tau \to 0$) divergences.[12] The divergences, as some $P^+ \to 0$, are associated with tachyon and

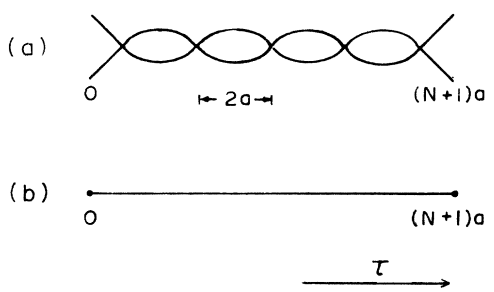

FIG. 8. (a) The bare open-string propagator carrying only 2 units of P^+. (b) The bare open-strong propagator carrying only one unit of P^+.

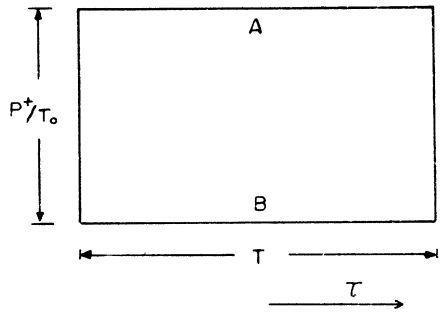

FIG. 9. The continuum limit of the open-string propagator.

zero-mass intermediate states and cannot be handled in models where the tachyon is present. There seems to be at least one dual model with no tachyon, although there are still massless particles.[13]

We shall compute a few simple processes in the DLE in Sec. III. In the remainder of this section we discuss the remaining field theory graphs not included in the conventional dual loop expansion.

D. Finite-momentum constituents in the dual string expansion

All the graphs not included in the DLE are characterized by at least one line carrying more than the minimal amount of P^+. For example, Fig. 15 has a line carrying three units of P^+. Of course, if such lines carry only a few units of P^+ they will only have microscopic effects, and in the continuum limit will only renormalize T_0. The effect will be macroscopic if a line carries a *finite fraction* of the total P^+ entering the graph.

We continue to follow our topological strong-coupling expansion; that is, we first consider the con-

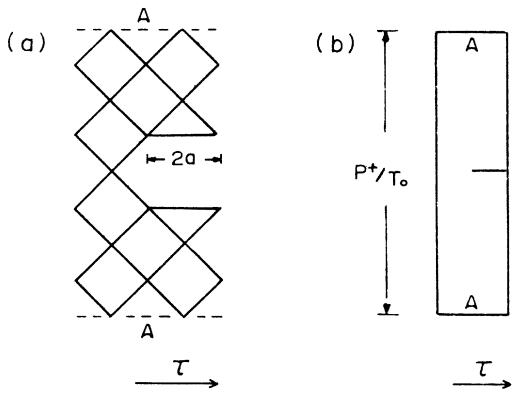

FIG. 10. (a) The vertex for the transition closed string → open string and (b) its continuum limit. Note that lines labeled by the same letter are identified.

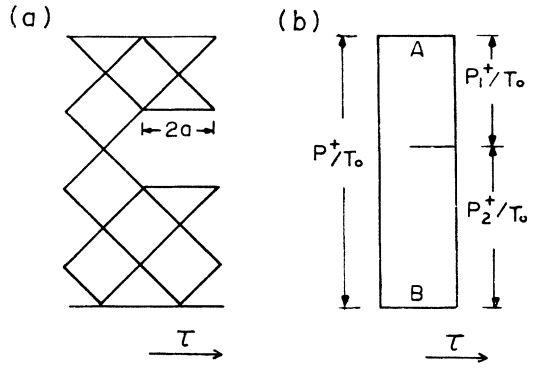

FIG. 11. (a) The vertex for the transition one open string → 2 open strings and (b) its continuum limit. Note that lines labeled by the same letter are identified.

tribution of these graphs to the sum of planar graphs, and within these we order the graphs according to a strong-coupling expansion. Our motivation is that this organizing principle maintains at each order in the expansion Lorentz invariance, crossing symmetry, good high-energy behavior, and perturbative unitarity with respect to a bare particle spectrum given by the excited states of open and closed strings.

So let us consider the planar graphs which have a maximum number of vertices given the constraint that one line carry $K<M$ units of P^+. To maximize the number of vertices in the graph as a whole, most of the time every line must carry minimal P^+. To achieve this the line carrying K units of P^+ must quickly degrade its momentum as shown in Fig. 16. The number of time steps this P^+ degradation takes is roughly $(\ln K)/\ln 3$. In the continuum limit with $M/N, K/M$ fixed, this time goes to zero like $(\ln K)/K$. We should then draw the continuum graph

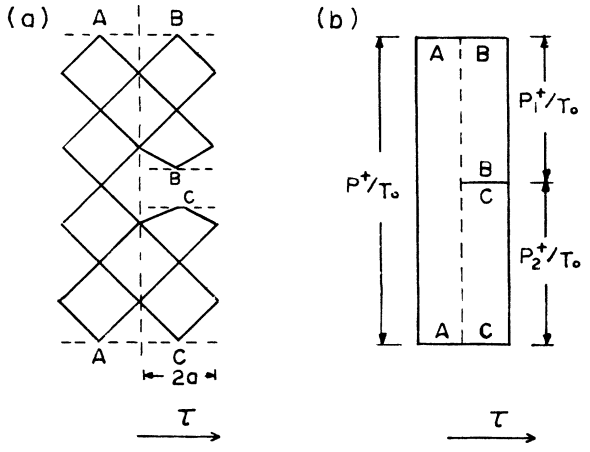

FIG. 12. (a) The vertex for the transition one closed string → 2 closed strings and (b) its continuum limit. Note that lines labeled by the same letter are identified.

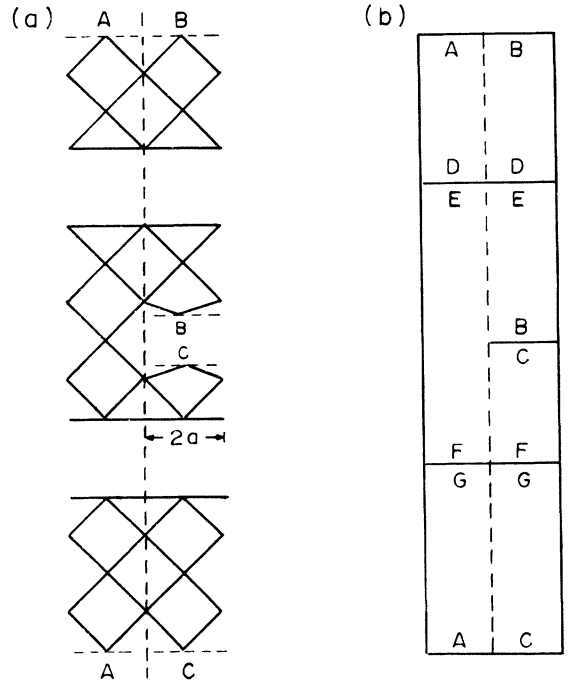

FIG. 13. (a) The vertex for the transition two open strings → two open strings and (b) its continuum limit. Note that lines labeled by the same letter are identified.

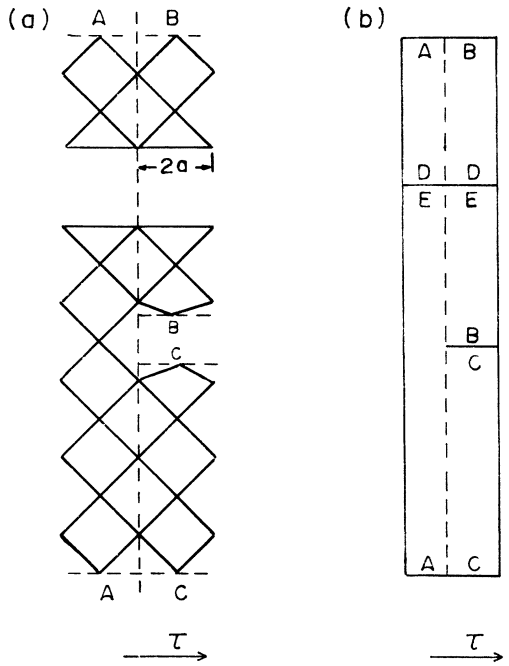

FIG. 14. (a) The vertex for the transition one open string → one closed and one open string and (b) its continuum limit. Note that lines labeled by the same letter are identified.

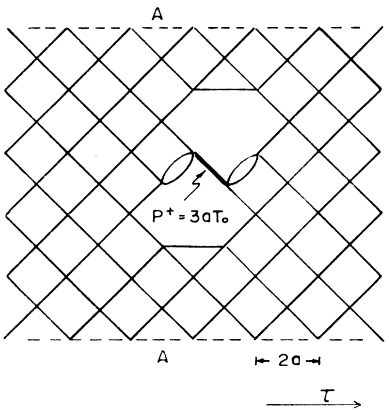

FIG. 15. A graph for the closed-string propagator with a single line carrying three units of P^+.

as in Fig. 17. That is, we draw the point-energy-density graphs of Green.[10] The line carrying K units of P^+ in the lattice graph goes in the continuum limit to a line segment on the light-cone string graph at fixed τ and of length KaT_0 equal to the total (macroscopic) amount of P^+. As this is a single line in the Feynman graph, the string coordinate $\vec{x}(\sigma,\tau)$ will be constant along this segment, i.e., $\partial\vec{x}/\partial\sigma = 0$ on this segment. Of course, the vertical and horizontal position of this line segment must be summed over.

If we follow our topological strong-coupling expansion, we should organize these nonminimal P^+ diagrams in the following way. First, calculate

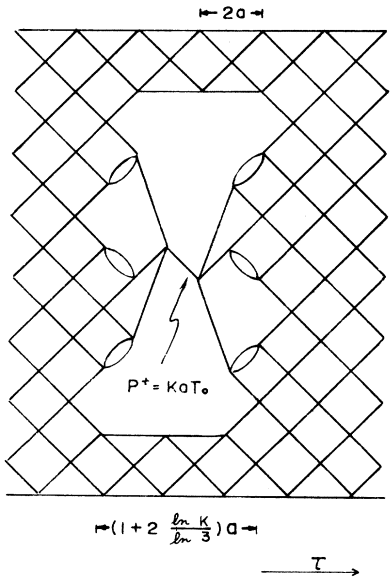

FIG. 16. A typical graph with a line carrying $K = 9$ units of P^+. Note that the lifetime of a nonminimal P^+ line is roughly $(\ln K/\ln 3)a$.

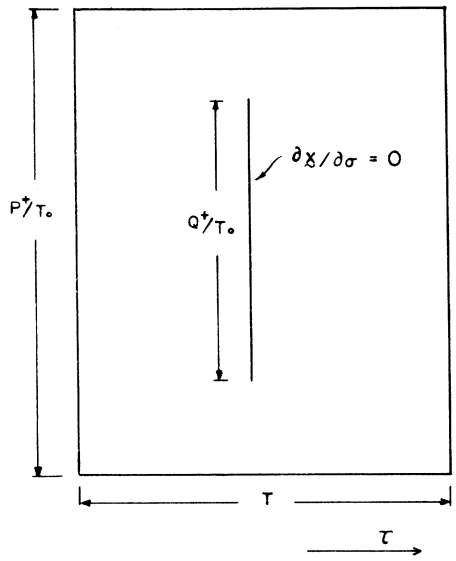

FIG. 17. The continuum limit of Fig. 16: M, N, $K \to \infty$ with $(N+1)/M = TT_0/P^+$, $K/M = Q^+/P^+$ fixed.

the effect of a single pointlike insertion on a planar graph. Then calculate any finite number of pointlike insertions separated by macroscopic distances, and integrate over their positions and sizes on the light-cone string diagram. The singularities associated with the collision of pointlike insertions among themselves or with holes is in principle regulated by the lattice cutoff. To show that this procedure does not introduce dependence of macroscopic effects on the microscopic fish-net structure, which is required to maintain Lorentz invariance, one must prove that as far as macroscopic phenomena are concerned, all lattice dependence is lumped into a renormalization of the rest tension T_0. If this can be shown, the dual string expansion, which is the conventional DLE, augmented by pointlike energy-momentum insertions, would yield a complete continuum theory that maintains order by order in the expansion all of the requirements of relativistic quantum theory.

Just as in the conventional field theory renormalization program, the expansion defined above cannot possibly be valid for all kinematic regions. This is because the effective expansion parameter changes via the renormalization group as one considers different mass scales. Specifically, our theory is $\mathcal{L}_I = \lambda\phi^4$ with $\lambda > 0$, i.e., an asymptotically free, infrared-unstable field theory. In such a theory, high-momentum processes correspond to $\lambda_{\text{eff}} \ll 1$ and strong coupling is appropriate, if at all, to the domain of low momenta (long distances). Our strong-coupling expansion is consistent with this association (q^2 small $\leftrightarrow$ λ large; q^2 large $\leftrightarrow$ λ small) in that the internal lines of our minimal P^+

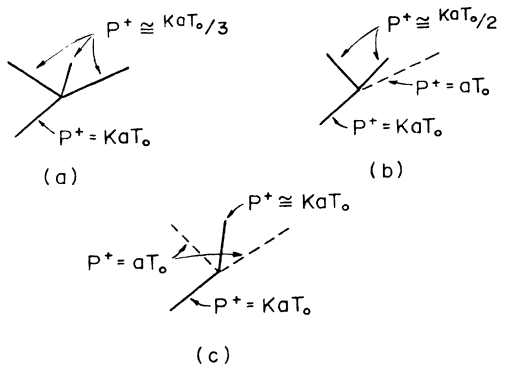

FIG. 18. Some four-point vertices with nonminimal P^+. The dashed lines carry the minimal $P^+ = a\,T_0$.

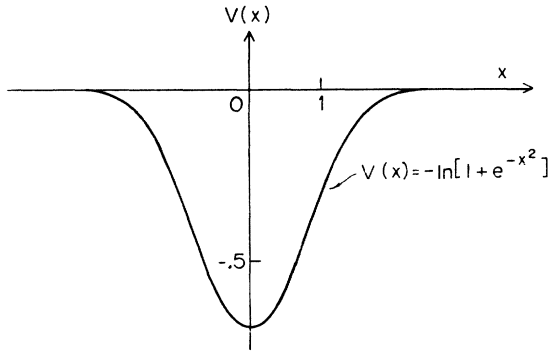

FIG. 19. The nearest-neighbor effective potential when missing vertices get positive weight.

fishnet diagram all carry infinitesimal momenta. However, the pointlike insertions involve lines carrying large momentum and the renormalization group tells us that effective vertices in which all legs carry high momentum are small. Thus, the vertex in Fig. 18(a) which carries high momentum in all legs should be suppressed by renormalization effects compared to 18(b) and 18(c). Thus it is possible that certain qualitative features gained using strong-coupling intuition, specifically the fact that a high-momentum constituent decays instantaneously into low-momentum constituents, will be drastically altered in the complete theory: Asymptotic freedom should slow this disintegration.

It is amusing to consider the reason we were forced into the asymptotically free situation $\lambda > 0$. This is the sign for which successive terms in perturbation theory of $\lambda\phi^4$ do not oscillate. We had to have this situation because the fishnet graphs are reinterpreted as interacting string graphs which are in turn functional integrals over $e^{-W_{\text{string}}} > 0$. If the corresponding graphs alternated in sign, this would correspond to complex contributions to W_{string}.

Another version of this observation is to think in terms of the missing links in the work of Giles and Thorn, the absence of a link getting a weight 1 and the presence of a link getting a weight $K\exp[-\frac{1}{2}T_0 \times (\Delta\vec{x})^2]$. The sum of these two possibilities is

$$1 + K\exp[-\tfrac{1}{2}T_0(\Delta\vec{x})^2] \equiv \exp[-V_{\text{eff}}(\Delta\vec{x})]$$

or

$$V_{\text{eff}}(\vec{x}) = -\ln[1 + K\exp(-\tfrac{1}{2}T_0\vec{x}^2)].$$

$K > 0$ reflects nonoscillation, while $K < 0$ reflects oscillations. Clearly the former represents an attractive potential (Fig. 19), whereas the latter represents a repulsive potential (Fig. 20). Our string can be thought of as many constituents interacting via a potential V_{eff}. Clearly the system should not bind for $K < 0$, whereas there is a chance for binding if $K > 0$.

The absence of sign oscillations is also responsible for asymptotic freedom. For if there are no oscillations, the lowest-order correction to a vertex is positive and hence has momentum dependence

$$\lambda \ln\frac{\Lambda^2}{q^2}, \quad q^2 \ll \Lambda .$$

$\ln\Lambda$ renormalizes λ and the effective coupling behaves as

$$\lambda_r\left(1 - \lambda_r \ln\frac{q^2}{M^2}\right)$$

and diminishes in strength as $q^2 \to \infty$.

In a realistic asymptotically free theory with positive energy density, like non-Abelian gauge theories, the situation is not so simple. For there are some attractive couplings and some repulsive couplings. We know the theory is asymptotically free at large q^2. We also know from work on perturbation theory at large orders[14] that the sum of *all* (planar and nonplanar) graphs at large order do *not* oscillate. Thus the situation looks hopeful for

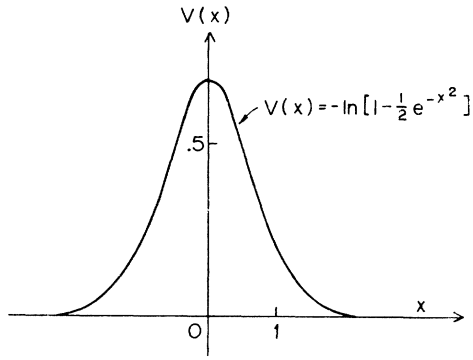

FIG. 20. The nearest-neighbor effective potential when a missing vertex gets negative weight.

a string or at least an extended object reinterpretation of QCD. We might remark that the planar diagrams we have been considering, while simple to calculate, may be only suggestive of a qualitative tendency for the constituents to bind into an extended object. If nonplanar diagrams are important this extended object may have width and perhaps resemble more nearly a bag for low-lying states.

III. SOME SIMPLE GRAPHS IN THE DUAL LOOP EXPANSION

In this section we describe in some detail the calculation of the bare string propagators and a simple transition amplitude. These calculations parallel the lattice string calculations of Giles and Thorn[9] so we concentrate attention on the differences. In the following we specialize to massless $\lambda\phi^4$ theory.

A. The closed-string propagator (Fig. 2)

Each line of the graph contributes a factor

$$\left(\frac{T_0}{2\pi}\right)^{d/2}\exp[-\tfrac{1}{2}T_0(\vec{x}-\vec{y})^2] \tag{3.1}$$

and each vertex a factor

$$\frac{\lambda}{8\pi T_0}\int d\vec{x}_\perp . \tag{3.2}$$

It is convenient to scale $\vec{x}\to(2\pi/T_0)^{1/2}\vec{x}$ and associate the factor $[(T_0/2\pi)^{1/2}]^d$ in (3.1) with vertex factors to get

$$\exp[-\pi(\vec{x}-\vec{y})^2] \tag{3.1'}$$

and

$$\frac{\lambda}{16\pi^2}\left(\frac{T_0}{2\pi}\right)^{(d/2)-1}\int d\vec{x}_\perp . \tag{3.2'}$$

The combination $(\lambda/16\pi^2)(T_0/2\pi)^{(d/2)-1}$ is dimensionless and we shall name it λ_0:

$$\lambda_0 \equiv \frac{\lambda}{16\pi^2}\left(\frac{T_0}{2\pi}\right)^{(d/2)-1} . \tag{3.3}$$

The vertices on the lines $\tau=0$ and $\tau=(N+1)a$ are "half" vertices, and if we associate $\lambda_0^{1/2}$ with each, closure will be simply integration over $\vec{x}$ with unit weight. We therefore have

$$\mathfrak{D}_{\text{closed string}}=\lambda_0^{(M/2)(N+1)}\int\prod_{ij}d\vec{x}_{ij}\exp\left[-\pi\left(\sum_{ij}(\vec{x}_{ij+1}-\vec{x}_{ij})^2+\sum_{i,j,}(\vec{x}_{i-1j+1}-\vec{x}_{ij})^2+\sum_{i,j}(\vec{x}_{i+1,j+1}-\vec{x}_{ij})^2\right)\right], \tag{3.4}$$

where $\vec{x}_{i0}$, $\vec{x}_{i,N+1}$ are held fixed.

Just as in Giles and Thorn[9] it is best to transform to normal-mode coordinates ($K=\frac{1}{2}M$ which we take odd for simplicity):

$$\vec{x}_{ij}=\frac{1}{\sqrt{K}}\vec{q}_{0j}+\sum_{m=1}^{(K-1)/2}\left(\frac{2}{K}\right)^{1/2}\left(\vec{q}^{\,c}_{mj}\cos\frac{2m\pi}{K}(i-\tfrac{1}{2})+\vec{q}^{\,s}_{mj}\sin\frac{2m\pi}{K}(i-\tfrac{1}{2})\right) . \tag{3.5}$$

This decomposition does not completely diagonalize the action and a further rotation of the odd modes is necessary:

$$\vec{q}^{\,c,s}_{mj}\to\cos\frac{m\pi}{K}\vec{q}^{\,c,s}_{mj}\pm\sin\frac{m\pi}{K}\vec{q}^{\,s,c}_{mj}\quad(j\text{ odd}), \tag{3.6}$$

after which we obtain

$$\mathfrak{D}^{\text{closed}}=\lambda_0^{(M/2)(N+1)}\int\prod_{m,j,c,s}d\vec{q}_{mj}\exp\left\{-\pi\left[2\sum_j(\vec{q}_{0j+1}-\vec{q}_{0j})^2+2\sum_{j=0}^{N}\left(2\cos\frac{m\pi}{K}(\vec{q}^{\,c}_{mj+1}-\vec{q}^{\,c}_{mj})^2+(c\to s)\right)\right.\right.$$
$$\left.\left.+2\sum_{j=0}^{N}\left(1-\cos\frac{m\pi}{K}\right)[\vec{q}^{\,c2}_{mj+1}+\vec{q}^{\,c2}_{mj}+(c\to s)]\right]\right\}, \tag{3.7}$$

which we recognize as a path history sum for a collection of harmonic oscillators of various masses and spring constants. We quote the final result:

$$\mathfrak{D}^{\text{closed}} = \lambda_0^{(M/2)(N+1)} \prod_{m=1}^{(K-1)/2} \left(4\sin\frac{m\pi}{K}\right)^d \left(\frac{2}{N+1}\right)^{d/2} \exp\left\{-\tfrac{1}{2}(N+1)d\left[K\ln 2 + \sum_{n=1}^{K-1} \ln\left(1+\sin\frac{m\pi}{K}\right)\right]\right\}$$
$$\times \prod_{m=1}^{(K-1)/2} (1-e^{-(N+1)\lambda_m})^{-d}$$
$$\times \prod_{m,c,s} \exp\left[-2\pi\sin\frac{m\pi}{K}\left((\vec{q}_{mf}^{\,2}+\vec{q}_{mi}^{\,2})\coth\lambda_m(N+1) - 2\vec{q}_{mf}\cdot\vec{q}_{mi}\,\frac{1}{\sinh\lambda_m(N+1)}\right)\right], \tag{3.8}$$

where $\lambda_m = \cosh^{-1}[1/\cos(m\pi/K)]$.

B. The closed-string partition function

We obtain the partition function for the closed string by identifying q_i and q_f in (3.8) and integrating. The result is

$$Z^{\text{closed}}(M, N+1) = \lambda_0^{(M/2)(N+1)} L_0^d \left(\frac{2}{N+1}\right)^{d/2} \exp\left\{-\frac{N+1}{2} d\left[K\ln 2 + \sum_{m=1}^{K-1} \ln\left(1+\sin\frac{m\pi}{K}\right)\right]\right\}$$
$$\times \prod_{m=1}^{(K-1)/2} \frac{1}{(1-e^{-(N+1)\lambda_m})^{2d}}$$
$$\underset{M,N\to\infty}{\sim} \lambda_0^{(M/2)(N+1)} L_0^d \left(\frac{2}{N+1}\right)^{d/2} \exp\left(-\frac{(N+1)MG}{\pi} d + \frac{\pi(N+1)}{6M} d\right)$$
$$\times \prod_{m=1}^{\infty} \{1-\exp[-(2m\pi/M)(N+1)]\}^{-2d}. \tag{3.9}$$

In this formula

$$G = \sum_{n=0}^{\infty} \frac{(-1)^n}{(2n+1)^2}$$

is Catalan's constant and $L_0 = \int dq_0$ is the volume of q_0 space. Because $x_{\text{c.m.}} = \sqrt{K}\, q_0$ by (3.5), $L_0 = (\frac{1}{2}M)^{1/2} L$ where L is the volume of $x_{\text{c.m.}}$ space. By using the Jacobi imaginary transformation[15] one can easily verify that the coefficient of L^d is symmetric under the interchange $(M \leftrightarrow N+1)$ (duality).

From (3.9) one can deduce the P^- levels of the closed string. The excitations are

$$(P_m^- - P_G^-)^{\text{closed}} = \frac{1}{a}\frac{2m\pi}{M} = \frac{2\pi T_0 m}{P^+} \equiv \frac{M_m^{c2} - M_G^{c2}}{2P^+}$$

from which we obtain

$$M_m^{c2} - M_m^{s2} = 4\pi T_0 m \tag{3.10}$$

and also

$$P_0^{-\,\text{closed}} = \frac{dMG}{\pi a} - \frac{M}{2a}\ln\lambda_0 - \frac{\pi d}{6Ma}. \tag{3.11}$$

As discussed by Giles and Thorn[9] the terms proportional to M are unobservable because they cancel out of all measurable energy differences. They can therefore be dropped and we are left with

$$M_G^{c2} = -\frac{2\pi\tau_0 d}{6} \tag{3.12}$$

the familiar tachyon.

C. The open-string partition function

This quantity is Fig. 6 with the initial and final coordinates identified and integrated over. The simplest way to calculate it is to recognize that with the interchange of the roles of M and $N+1$, it is identical to the closed-string propagator evaluated between particular initial and final states.[16] We only need identify the appropriate states. A little thought shows that the states are those with zero momentum density, i.e., q_{im} and q_{fm} integrated independently with constant weight. However, the factors $\lambda_0^{1/2}$ are omitted from the initial and final vertices.

So we first integrate (3.8) over q_{mi} and q_{mf} and multiplying by $\lambda_0^{-M/2}$ gives

$$Z^{\text{open}}(N+1,M)=\lambda_0^{-M/2}\lambda_0^{(M/2)(N+1)}L_0^{d}\prod_{m=1}^{(K-1)/2}\left(\frac{1}{\sin(m\pi/K)}\right)^{d}$$
$$\times\exp\left\{-\left(\frac{N+1}{2}\right)d\left[\frac{M}{2}\ln 2+\sum_{m=1}^{M/2-1}\ln\left(1+\sin^2\frac{m\pi}{M}\right)\right]\right\}\prod_{m=1}^{(K-1)/2}(1-e^{-2(N+1)\lambda_m})^{-d}$$
$$\underset{M,N\to\infty}{\sim} L_0^{d}\left(\frac{1}{M}\right)^{d/2}2^{Md/4}\lambda_0^{-M/2}\exp\left[-(N+1)M\left(\frac{Gd}{\pi}-\tfrac{1}{2}\ln\lambda_0\right)+\frac{\pi d(N+1)}{6M}\right]$$
$$\times\prod_{m=1}^{\infty}\{1-\exp[-4(N+1)m\pi/M]\}^{-d}. \tag{3.13}$$

Recalling that $L_0=L(M/2)^{1/2}$ we have [interchanging $M\leftrightarrow(N+1)$],

$$Z^{\text{open}}(M,N+1)\sim L^{d}\left(\frac{1}{2}\right)^{d/2}\left(\frac{\lambda_0}{2^{d/2}}\right)^{-(N+1)/2}\exp\left[-(N+1)M\left(\frac{Gd}{\pi}-\tfrac{1}{2}\ln\lambda_0\right)+\frac{\pi dM}{6(N+1)}\right]$$
$$\times\prod_{m=1}^{\infty}\{1-\exp[-4Mm\pi/(N+1)]\}^{-d}$$
$$=L^{d}\left(\frac{M}{N+1}\right)^{d/2}\exp\left\{-(N+1)\left[M\left(\frac{6d}{\pi}-\tfrac{1}{2}\ln\lambda_0\right)+\tfrac{1}{2}\ln\frac{\lambda_0}{2^{d/2}}-\frac{\pi d(N+1)}{24M}\right]\right\}$$
$$\times\prod_{m=1}^{\infty}\{1-\exp[-(N+1)m\pi/M]\}^{-d}, \tag{3.14}$$

where the last equality follows after a Jacobi imaginary transformation.

Thus the open-string excitation spectrum is

$$(P_m^- - P_G^-)^{\text{open}}=\frac{2\pi T_0 m}{2P^+}$$

or

$$M_m^{02}-M_G^{02}=2\pi T_0 m \tag{3.15}$$

with

$$P_G^{-\,\text{open}}=\frac{M}{a}\left(\frac{Gd}{\pi}-\tfrac{1}{2}\ln\lambda_0\right)+\frac{1}{2a}\ln\frac{\lambda_0}{2d/2}-\frac{\pi dT_0}{24P^+}. \tag{3.16}$$

Since only energy differences are significant we compare with $P_G^{-\text{closed}}$:

$$P_G^{-\,\text{open}}-P_G^{-\,\text{closed}}=\frac{1}{2a}\ln\frac{\lambda_0}{2^{d/2}}-\frac{2\pi T_0 d}{2P^+}\left(\tfrac{1}{24}-\tfrac{1}{6}\right). \tag{3.17}$$

We see from (3.17), that the open string will have a finite (and covariant) P^- compared to the closed string only if

$$\lambda_0=2^{d/2}\equiv\lambda_0^{\text{critical}} \tag{3.18}$$

or

$$\lambda=32\pi^2\left(\frac{4\pi}{T_0}\right)^{d/2-1}\equiv\lambda^{\text{critical}} \tag{3.19}$$

If $\lambda<\lambda^{\text{critical}}$ the open string has an infinitely lower P^- than the closed string in the continuum limit, so the lowest state would be noncovariant. If $\lambda>\lambda^{\text{critical}}$ the open string will gain an infinite P^- compared to the closed string. Thus although the expression (3.17) is not covariant, this fact will not be important.

However, it is only for $\lambda=\lambda^{\text{critical}}$ that the full dual loop expansion involving both open and closed strings exists. If we accept this eigenvalue condition on λ, the DLE is characterized by only one free parameter, T_0, which replaces the only free parameter λ in the original ϕ^4 field theory. This is similar to dimensional transmutation. The number of free parameters in the string expansion of field theory is identical to the number of free parameters in the weak-coupling expansion of field theory, though the free parameters play different roles in the two expansions.

D. The closed-string–open-string vertex: The critical dimension

We shall not go through this calculation, and we refer the reader to Appendix B of Giles and Thorn.[9] The Giles-Thorn calculation was for a rectangular grid rather than our diamond array. The vertex for ground states was found to behave like

$$V_{\text{closed-open}} \underset{M\to\infty}{\sim} \frac{(K')^d}{M^{d/16}} \tag{3.20}$$

and it was shown that only for $d=24$ did diagrams containing these vertices have a finite continuum limit. It is clear from the Giles-Thorn calculation that the power of M in (3.20) depends only on the low-lying spectrum and the long-wavelength structure of the string wave functions. As the diamond array has an identical long-wavelength structure, the same power will come out of the fishnet calculation. The *coefficient* of $1/M^{d/16}$ will be different, but nonetheless *finite and calculable* It is the size of this coefficient which controls the size of higher-order corrections in the dual loop expansion. It is evident that the fishnet dual loop expansion requires the same critical dimension as the lattice string DLE.

IV. CONCLUDING REMARKS

Let us take stock of what we have achieved in this work. Utilizing a novel lattice we have rewritten the entire Feynman graph series for $\lambda\phi^4$ field theory as a dual string expansion, which is a combined topological and strong-coupling expansion. This expansion has features in common with both $1/N$ expansions and straight strong-coupling expansions. It has the virtue that each order can be calculated and the continuum limit can be explicitly taken to each order in the expansion.

To finite order in the expansion, and for critical values of couplings and dimensions, this expansion is explicitly (1) Lorentz covariant, (2) crossing symmetric, (3) power behaved at large energies, and (4) perturbatively unitary with respect to a bare particle spectrum given by the excited states of open and closed relativistic strings. The subset of graphs which give the dual loop expansion satisfy Regge behavior. That is, the expansion obeys order by order the same requirements put on standard field-theoretic perturbation theory. We regard these properties as highly nontrivial.

This reinterpretation of the Feynman series requires the "wrong" sign of the coupling λ. The reason is that successive terms in the series cannot oscillate in sign, and in a theory as simple as ϕ^4 theory this can only be arranged with a negative potential term $V(\phi)$. This nonoscillation is also reponsible for the asymptotic freedom of wrong-sign ϕ^4 theory. Since the theory is asymptotically free, one can, in principle, check whether the string interpretation is the same theory by seeing if high-momentum, short-distance, phenomena are controlled by weak-coupling perturbation theory. The string reinterpretation should only alter long-distance (low-momentum) phenomena.

QCD, a much more complicated theory, has similar features to wrong-sign ϕ^4 theory, namely, asymptotic freedom, and nonoscillation of large orders in perturbation theory. (This latter feature is known only for the sum of *all* large-order graphs including nonplanar ones). Further, QCD has a positive energy density, unlike wrong-sign ϕ^4 theory. We tentatively associate the dual tachyon with the negative energy density of wrong-sign ϕ^4 theory and hope that QCD will not have this problem. We remarked that the string reinterpretation of QCD will not be as simple and straightforward as in wrong-sign ϕ^4 since there are both attractive and repulsive couplings. The hope is that the attractive couplings win at large distances and bind many gluons into an extended object, but that the repulsive couplings help the expansion avoid the tachyon problem.

ACKNOWLEDGMENTS

This exposition benefited from conversations with C. DeTar, R. Giles, J. Goldstone, F. E. Low, and L. McLerran, and their comments and suggestions are gratefully acknowledged. This work was supported in part through funds provided by ERDA under Contract No. EY-76-C-02-3069.*000 and the Alfred P. Sloan Foundation.

[1]C. B. Thorn, Phys. Lett. 70B, 85 (1977).
[2]For a slightly different approach to fishnet diagrams, see K. Bardakci and S. Samuel, Phys. Rev. D 16, 2500 (1977).
[3]H. B. Nielsen and P. Olesen, Phys. Lett. 32B, 203 (1970); B. Sakita and M. A. Virasoro, Phys. Rev. Lett. 24, 1146 (1970).
[4]For a collection of excellent reviews see, for example, *Dual Theory*, edited by M. Jacob (North-Holland, Amsterdam, 1974).
[5]P. Goddard, J. Goldstone, C. Rebbi, and C. B. Thorn, Nucl. Phys. B56, 104 (1973).
[6]S. Mandelstam, Nucl. Phys. B64, 461 (1974); B83, 413 (1974).
[7]G. 't Hooft, Nucl. Phys. B72, 461 (1974).
[8]G. Veneziano, Phys. Lett. 52B, 220 (1974); Nucl. Phys. B74, 365 (1974); B117, 519 (1976); G. 't Hooft, *ibid.* B75, 461 (1974); G. C. Rossi and G. Veneziano, *ibid.* (to be published).
[9]R. Giles and C. B. Thorn, Phys. Rev. D 16, 366 (1977).
[10]M. B. Green, Phys. Lett. 69B, 89 (1977).
[11]J. Kogut and D. E. Soper, Phys. Rev. D 1, 2901 (1970);

J. D. Bjorken, J. Kogut, and D. E. Soper, *ibid*. 3, 1382 (1971).
[12]M. Ademollo, A. D'Adda, R. D'Auria, F. Gliozzi, E. Napolitano, S. Sciuto, and P. D. DiVecchia, Nucl. Phys. B94, 221 (1975).
[13]F. Gliozzi, J. Scherk, and D. Olive, Phys. Lett. 65B, 282 (1976).
[14]L. N. Lipatov, Leningrad Nuclear Physics Institute report, 1976 (unpublished); E. Brézin, J. C. Le Guillou, and J. Zinn-Justin, Phys. Rev. D 15, 1544 (1977); 15, 1558 (1977).
[15]See, for example, *Higher Transcendental Functions* (Bateman Manuscript Project), edited by A. Erdélyi (McGraw-Hill, New York, 1953), Sec. 13.22.
[16]This calculation was done in collaboration with R. Giles and L. McLerran, in R. Giles, L. McLerran, and C. B. Thorn, Phys. Rev. D (to be published).